Improving the Delivery of Camptothecin through the Blood-Brain Barrier via Modulation of Paracellular Pathway using E-Cadherin Peptide

By

Kayann Tabanor

Submitted to the graduate degree program in Chemistry and the Graduate Faculty of the University of Kansas in partial fulfillment of the requirements for the degree of Master of Science

Committee:

_____

Chairman: Dr. Jon Tunge

_____

Dr. Helena Malinakova

_____

Dr. Teruna J. Siahaan

Date Defended: September 9th, 2014

The Thesis Committee for Kayann Tabanor

certifies that this is the approved version of the following thesis:

Improving the Delivery of Camptothecin through the Blood-Brain Barrier via Modulation of Paracellular Pathway using E-Cadherin Peptide

_____

Chairman: Dr. Jon Tunge

Date Defended: September 9th, 2014

Improving the Delivery of Camptothecin through the Blood-Brain Barrier via Modulation of Paracellular Pathway using E-Cadherin Peptide

Kayann Tabanor

Abstract

The successful treatments of brain tumors and many other brain disorders have been limited due to the presence of barricade from microvascular endothelium called the blood-brain barrier (BBB). It was estimated that over 98% of newly developed pharmaceutical drugs do not cross the BBB; therefore, it is necessary to develop methods to improve the delivery of drugs to the brain. In this investigation, we evaluated the ability of HAV6 peptide (Ac-SHAVSS-NH_2) to improve the paracellular transport of Camptothecin-glutamate (CPT-Glu) across the BBB using an *in-situ* rat brain perfusion model. CPT-Glu was synthesized through conjugation between an anti-cancer drug camptothecin (CPT) and L-glutamic acid via an ester bond to improve its solubility. A perfusate containing CPT-Glu (10 mg/kg) and 1.0 mM HAV6 peptide was delivered to the brain of anesthetized Sprague Dawley rats using the *in-situ* brain perfusion technique. Accumulation in the brain was determined through acidic extraction of CPT-Glu and its hydrolyzed product CPT from harvested brain, followed by detection using LC-MS/MS. The extraction and LC-MS/MS detection methods have been successfully developed to detect 0.25 and 17 ng/mL CPT and CPT-Glu respectively. Both CPT-Glu and CPT were successfully detected in the rat brains after *in-situ* brain perfusion in the absence and presence of HAV6 peptide. Rats perfused with CPT-Glu in combination with HAV6 had higher deposition of drug in the brain compared to CPT-Glu alone. The HAV6 treated rats had 650.85 ng of CPT equivalent delivered per gram of brain (1.30-fold) compared to 498.40 ng/g in control. The results also showed that CPT-Glu conjugate was hydrolyzed to CPT in the brain after delivery. In future studies, HAV6 peptide perfusion time will be extended for receptor saturation to promote effective BBB opening. The concentration of CPT-Glu will be increased to enhance delivery and improve detection in the brain.

TABLE OF CONTENT

Page

1. INTRODUCTION

Many potential drugs developed for the treatment of diseases of the central nervous system (CNS) such as neurodegenerative diseases, brain tumors and infections of the brain have failed during development due to their poor brain absorption. The poor absorption could be attributed to the presence of the blood-brain barrier (BBB) and/or unfavorable physical-chemical properties of the drug for penetrating the BBB [1]. The BBB is located between the systemic blood circulation and the brain. It is a highly selective barrier whose main function is to regulate the passage of nutrients into brain and provides protection against toxic compounds and pathogens [2, 3]. The BBB is comprised of endothelial cells that make the blood capillaries in the brain [4]. The transcellular transport of drug molecules is limited due to the unfavorable physicochemical properties of drug molecules and the presence of efflux pumps [4-7]. Paracellular passage of drugs is limited due to the presence of intercellular tight junctions [7]. Intercellular tight junctions are composed of tight junctions (TJs) and adherens junctions (AJs). Within the TJs are complex proteins such as occludins and claudins. AJs cadherin proteins span the intercellular cleft and are linked into the cell cytoplasm by the scaffolding proteins alpha, beta and gamma catenin [5, 8]. The AJs hold cells together giving the tissue structural support. They are essential for formation of tight junction and disruption of AJs leads to paracellular barrier disruptions [5, 8]. E-cadherins are a family of transmembrane glycoproteins found in the AJs and they mediate specific cell-cell adhesion in the opposing cells. These Ca^{2+}-dependent proteins are comprised of five extracellular repeats (EC1 to EC5) that form a *cis*-dimer between two E-cadherin molecules in the same cell [9].

Here, our overall goal is to improve the paracellular delivery of an anticancer drug molecule (Camptothecin (CPT)). This is achieved by delivering a combination of CPT and an HAV6

peptide (Ac-SHAVSS-NH_2). The HAV6 peptide was derived from the EC1 domain of E-cadherin and have been shown modulate the intercellular junctions of the *in vitro* and *in vivo* models of the BBB. CPT is a naturally occurring alkaloid extracted from the *camptotheca acuminata* plant that exhibits antitumor activity in various cancers. CPT suppresses cancer proliferation by inhibiting topoisomerase-I, an enzyme required for replication and transcription of cancer cells [10-14]. Despite its promising anticancer activity, the utility of CPT in cancer therapeutic has been severely hampered due to its unfavorable physicochemical properties. First, CPT has very poor aqueous solubility (2.5 μg/mL), making it difficult to formulate and deliver [14]. Second, CPT undergoes lactone hydrolysis under physiological conditions (pH 7.4) to produce the carboxylate form (Scheme 1). CPT-carboxylate is known to readily bind human serum albumin (HSA) which lowers the concentration of active CPT-lactone (stable at pH <5.5) in bloodstream [13, 15-17]. Despite these drawbacks, several analogs such as topotecan (Hycamtin®) and irinotecan (Campto®) have been developed to improve solubility and pharmacokinetic profiles [10]. These CPT-derivatives have been approved to treat various forms of ovarian, cervical and lung cancers [10].

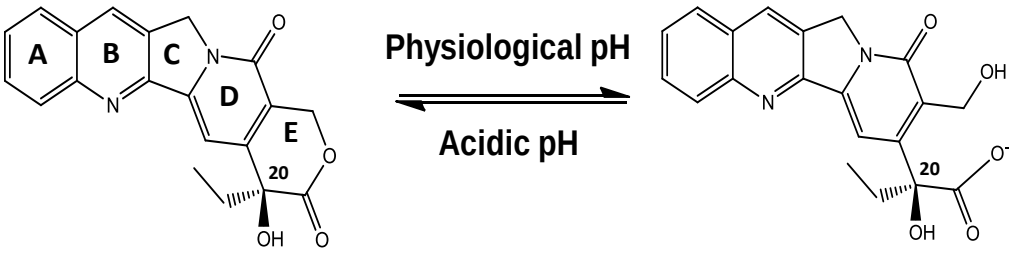

Scheme 1. Structure of camptothecin and pH dependent equilibrium between lactone (closed ring, left) and carboxylate (open ring, right) form of the drug.

Our group developed H-A-V (His-Ala-Val) and A-D-T (Ala-Asp-Thr) peptides that can modulate cadherin-cadherin interactions at the intercellular junctions to promote the passage of

drug molecules through the paracellular pathway of the BBB [9, 18-20]. HAV and ADT peptides derived from EC1 domain of E-cadherin were used in *in-vitro* BBB models to evaluate their efficacies on paracellular porosity. These peptides have been shown to inhibit aggregation of single cells of bovine brain microvessel endothelial cells (BBMECs) and to increase the permeability of Madin-Darby canine kidney (MDCK) cell monolayers as reflected by lowering transepithelial electrical resistance (TEER) values and increasing paracellular permeation of ^{14}C-mannitol [9, 18-20]. Further studies using an HAV6 peptide was found to enhance the paracellular permeation of anticancer drug ^{3}H(G)-daunomycin and ^{14}C-mannitol across the BBB in an *in-situ* brain perfusion rat model [21]. More recently, HAV6 has been shown to enhance *in-vivo* delivery of gadolinium diethylenetriaminepentaacetate (Gd-DTPA) and rhodamine 800 (R800) [22]. Gd-DTPA and R800 are a magnetic resonance imaging (MRI) contrast agent and a near IR dye for fluorescent imaging, respectively.

CPT is a very insoluble molecule, which is difficult to delivery in high dose. The lactone ring on CPT is essential for the anticancer activity; however, it is unstable and undergoes hydrolytic reaction (Scheme 1). To improve its stability, the 20-OH has been conjugated to different moieties to stabilize the lactone ring as well as improving solubility and pharmacokinetic profiles of CPT [13, 14, 23, 24]. Here, we synthesized camptothecin-glutamate (CPT-Glu) via conjugation of the C-terminus of L-glutamic acid to the 20-OH group of CPT. The brain delivery of CPT-Glu conjugate was evaluated in the presence and absence of HAV6 peptide in the *in-situ* brain perfusion rat model. To detect the amount of CPT-Glu and CPT in the brain, the extraction method of CPT-Glu and CPT from the brain was developed. The liquid chromatography mass spectrometry/mass spectrometry (LC-MS/MS) method was also developed to quantitate the amount of compounds in the brain extract. The LC-MS/MS is a selective and sensitive method to

identify and quantify the CPT-Glu and CPT in the brain homogenate and it eliminates the need for radiolabeled compounds [25].

2. MATERIALS AND METHODS

2.1. Synthesis of Camptothecin-Glutamate (CPT-Glu) Conjugate

The conjugation of Camptothecin (CPT) to L-glutamic acid (CPT-Glu) was accomplished by forming an ester bond between the 20-OH group of CPT and the alpha-carboxylic acid group of the glutamic acid using previous methods with minor modifications (Scheme 2) [26, 27]. A suspension mixture of camptothecin (0.10 g, 0.288 mmol), scandium triflate (0.085 g, 0.173 mmol), N-Boc-L-glutamic acid gamma t-butyl ester (Aapptec Company, 0.524 g, 1.728 mmol) and N, N-dimethylaminopyridine (0.11 g, 0.864 mmol) in anhydrous dimethylformamide (DMF) (5 mL) was cooled to –8°C in salt water ice bath. 1, 3-Diisopropylcarbodiimide (0.142 mL, 0.907 mmol) was added slowly to the reaction, stirred at –8 °C for 30 min and allowed to warm to room temperature and react for 1 h. After completion, the reaction mixture was treated with water (50 mL) and extracted with 100 mL dichloromethane. The organic extract was washed sequentially with solutions of 0.1 M HCl (200 mL) and 0.1 M $NaHCO_3$ (200 mL), followed by water extraction. The organic layer was dried with sodium sulfate followed by evaporation under reduced pressure. The CPT-Boc-L-glutamic acid gamma t-butyl ester residue was treated with a solution of dichloromethane-trifluoroacetic acid (1:1, 2 mL) and stirred at room temperature for 1 h. The solvent was removed under reduced pressure and the resulting residue was purified by reverse-phase HPLC using a C_{18} preparative grade column followed by lyophilization to give CPT-Glu conjugate (0.90 g).

2.2. LC-MS/MS Method Development

2.2.1. Preparation of Stock and Standard Solutions

Stock solutions (1 mg/mL) of CPT, CPT-Glu and SN-38 were dissolved in dimethyl sulfoxide (DMSO) and stored at –20 °C. Working solutions of CPT and CPT-Glu were prepared prior to experiments by diluting stocks with acetonitrile:water (1:1 v/v). Final concentrations of CPT and CPT-Glu calibration standards were in the range between 5 and 500 ng/mL. SN-38 was used as an internal standard (IS). Calibration curves for both CPT and CPT-Glu were constructed by plotting the ratio of the peak area of the spike analyte and IS at each concentration. These standards were used to determine total concentration of CPT and CPT-Glu delivered to the brain of each rat. Working standards used for extraction recovery experiments were prepared by diluting stocks solutions in DMSO and phosphate buffer at pH 3 (1:1 v/v) before spiking in tissue homogenate.

2.2.2. Extraction Recovery from Brain Tissue Homogenate

Extraction recovery of CPT and CPT-Glu from brain tissue homogenate was determined by comparing the response from the analyte extracted from spiked homogenate to working standards of analyte spiked in blank extracts. Concentrations studied for each analyte were 50, 250 and 500 ng/mL. The brain of an untreated rat (blank) was homogenized and 190 μL aliquots of tissue homogenate were spiked with 10 μL of working standards for CPT and CPT-Glu. The mixture was vortexed for 1 min. A mixture of phosphate buffer at pH 3 and acetonitrile (1:6 v/v) was added to the homogenate; then, the mixture was vigorously vortexed for 1 min followed by centrifugation at 12000 rpm. The supernatant was isolated and transferred to a clean tube and

evaporated to dryness under nitrogen at 40 °C. The dry extract was reconstituted in 300 μL of 1:1 v/v acetonitrile:water with 0.1 % formic acid and vortexed for 30 sec. The samples were stored overnight at –20 °C; then, they were vortexed and centrifuge for 5 min at 12000 rpm to remove additional precipitated proteins. Each extract was spiked with 25 ng/mL IS before injection into LC-MS/MS.

2.2.3. Extraction of Drug from Brain Tissue after In-situ Brain Perfusion

A mixture (1:1 v/v) of phosphate buffer at pH 3 and 0.30 M phosphoric acid was added to each whole brain tissue with equal weight amount (1:1 w/w). The mixture was homogenized using a PowerGen 700 tissue homogenizer. Aliquots (250 μL) from rat brain homogenizes were treated with 1 mL of 0.30 M phosphoric acid and acetonitrile (1:6 v/v) and vortex vigorously for 1 min. Each homogenate was centrifuged at 12000 rpm for 5 min. The resulting supernatant was isolated and evaporated to dryness under nitrogen at 40 °C. The residue was resuspended in 300 μL of 1:1 v/v acetonitrile: water with 0.1 % formic acid. Samples were then stored overnight at –20 °C, and then, they were vortexed and centrifuged (12000 rpm for 5 min) to remove additional precipitated proteins before spiking with 25 ng/mL IS (SN-38). The sample (5 μL) was injected to LC-MS/MS.

2.2.4. Instrumentation and Chromatographic Conditions for LCMS/MS

The sample chromatography was performed on an Acquity UPLC system (Water Corp., Milford, MA, USA) with a temperature controlled autosampler set to 8 °C. Separation was performed at room temperature on a Luna UPLC C_{18} reversed-phase analytical column (2.1 mm

x 50 mm, 5 μm particle size, 100 Å; Phenomenex, Inc., Torrance, CA). A C_{18} guard cartridge (4 mm x 2 mm ID) was used to protect the main column. A gradient method was used to elute the analytes from the column. The mobile phases consisted of a binary gradient system composed of (A) H_2O:acetonitrile:formic acid (98.92:1:0.08) and (B) acetonitrile:H_2O:formic acid (98.92:1:0.08). Analytes were eluted using a gradient system of 15% B (initial), 15–30% B (2.5 min), 30–90% B (1 min), 90–15% B (0.5 min) and 15% B for 1 min. The eluent flow rate was 0.40 mL/min with 5 μL injection volumes with a total run time of 5 min.

On-line Mass Spectrometry (MS) detection was performed on a Quattro Ultima triple quadrupole mass analyzer (Micromass Ltd, Manchester, UK) equipped with an electrospray ionization (ESI) source coupled to the UPLC system. Data were acquired in multiple reaction monitoring (MRM) mode to monitor the characteristic pseudomolecular ion $[MH]^+$ of the compounds. Nitrogen was used as the desolvation gas and argon gas used for collision-induced dissociation (CID). All analytes were fragmented with cone voltage and collision energy set at 35V and 28V, respectively. MRM chromatograms were quantified using MassLynx v 4.1 software (Micromass UK Ltd) by integration of peaks.

2.3. In-Situ Brain Perfusion Technique for Delivery of CPT-Glu

The *in-situ* brain perfusion studies were done in adult male Sprague Dawley rats (250–350g) and the brain delivery of CPT-Glu was done in the presence and absence of HAV6 peptide as described by Takasato *et al*. with some modifications [28]. CPT-Glu was perfused in bicarbonate buffer (pH 7.4) containing 4.2 mM KCl, 1.5 mM $CaCl_2$, 0.9 mM $MgCl_2$, 128 mM NaCl, 2.4 mM NaH_2PO_4 and 24 mM $NaHCO_3$. Prior to the experiment, the perfusate was supplemented with D-

glucose (6 mM) followed by filtration and oxygenation upon incubation under 95% O_2 and 5% CO_2 at 37 °C. The rats were anaesthetized with a combination of ketamine (100 mg/kg) and xylazine (5mg/kg) delivered intraperitoneally. Then, the left common carotid artery (LCCA) was canulated with a polyethylene catheter (PE 50) containing heparinized saline (100 IU/mL) at artery for perfusion and prevent coagulation. The left pteryopalatine artery, occipital, and superior thyroid arteries were ligated using surgical thread. The animal body temperature was maintained with a heat lamp during the experiment.

Immediately after the heart was cut on the anaesthetized rat, the LCAA was washed with saline (10 sec) at 5 mL/min delivered with a syringe pump (Model 341 B, Sage Instruments). Then, the brains were perfused with 1.0 mM HAV6 in HCO_3 buffered physiological saline with 0.5 % Tween-20 at 5 mL/min for 10 mL. Then, 10 mL of a mixture of HAV6 (1.0 mM) and CPT-Glu (10 mg/kg) was perfused. Finally, a 10 sec post-perfusion wash with saline solution was delivered. The experiment was terminated by animal decapitation followed removal of the brain from skull. The whole brain was immediately stored in –80 °C until further use. A similar study was done using only CPT-Glu as a control.

Perfusion studies for control rats (CPT-Glu only) were performed similarly as described above. A 4 min perfusion of 10 mL HCO_3 buffer saline with 0.5% Tween-20 was followed by 10 mL of perfusate containing test compound CPT-Glu was done as a control.

3. RESULTS

3.1. Improving the Physical and Chemical Properties of Camptothecin (CPT)

The synthesis of CPT-Glu involved a two-step reaction in DMF as a solvent (Scheme 2). The alcohol group of CPT was coupled to a the alpha carboxylic acid of Boc-L-Glu(O-tBu)-OH and the protecting groups were used to prevent the side reactions. DIPC was used to activate the alpha carboxylic acid of the Glu amino acid. Then, the activated carboxylic acid was reacted to the 20-OH group of CPT in the presence of DMAP. This conjugation reaction generated a high yield of the desired product (> 90% yield); however, this reaction can lead to substantial epimerization [27]. The tert-butyl ester and Boc protecting groups were cleaved by 50% TFA in DCM to give the crude CPT-Glu. The crude CPT-Glu was purified using a reversed-phase C_{18} column to produce a pure conjugate. ^{1}H-NMR and mass spectrometry was used to analyze the HPLC purified product.

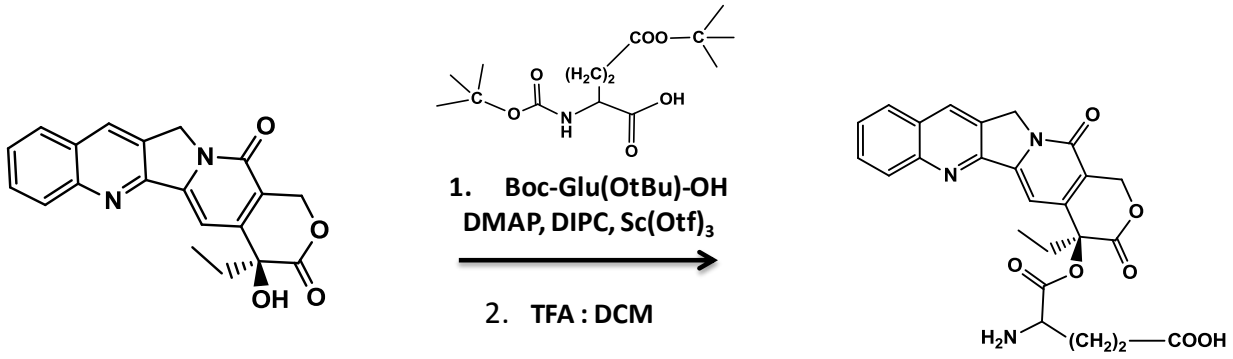

Scheme 2. Chemistry for conjugation of Camptothecin (CPT) to L-glutamic acid to make CPT-Glu.

3.2. Characterization of CPT-Glu by NMR and ESI-MS

After purification, CPT-Glu was characterized using ESI-MS and ^{1}H-NMR. ESI-MS data produced a dominant peak at m/z = 478.15 which corresponds with calculated molecular weight of CPT-Glu (Figure 1). The CPT-Glu was dissolved in DMSO-d6 and analyzed using Bruker Advance AV-III 500 NMR spectrometer (Figure 2). ^{1}H- NMR (DMSO-d6) δ 12.45 (s, 1H), 8.73 (s, 1H), 8.47 (s, 2H), 8.15 (d, 2H), 7.88 (m, 1H), 7.74 (t, 1H), 7.27 (s, 1H), 5.57 (s, 2H), 5.33 (s, 2H), 4.38 – 4.5 (s, 1H), 2.62 (m, 1H), 2.10 – 2.30 (m, 4H), 0.90 (t, 3H)

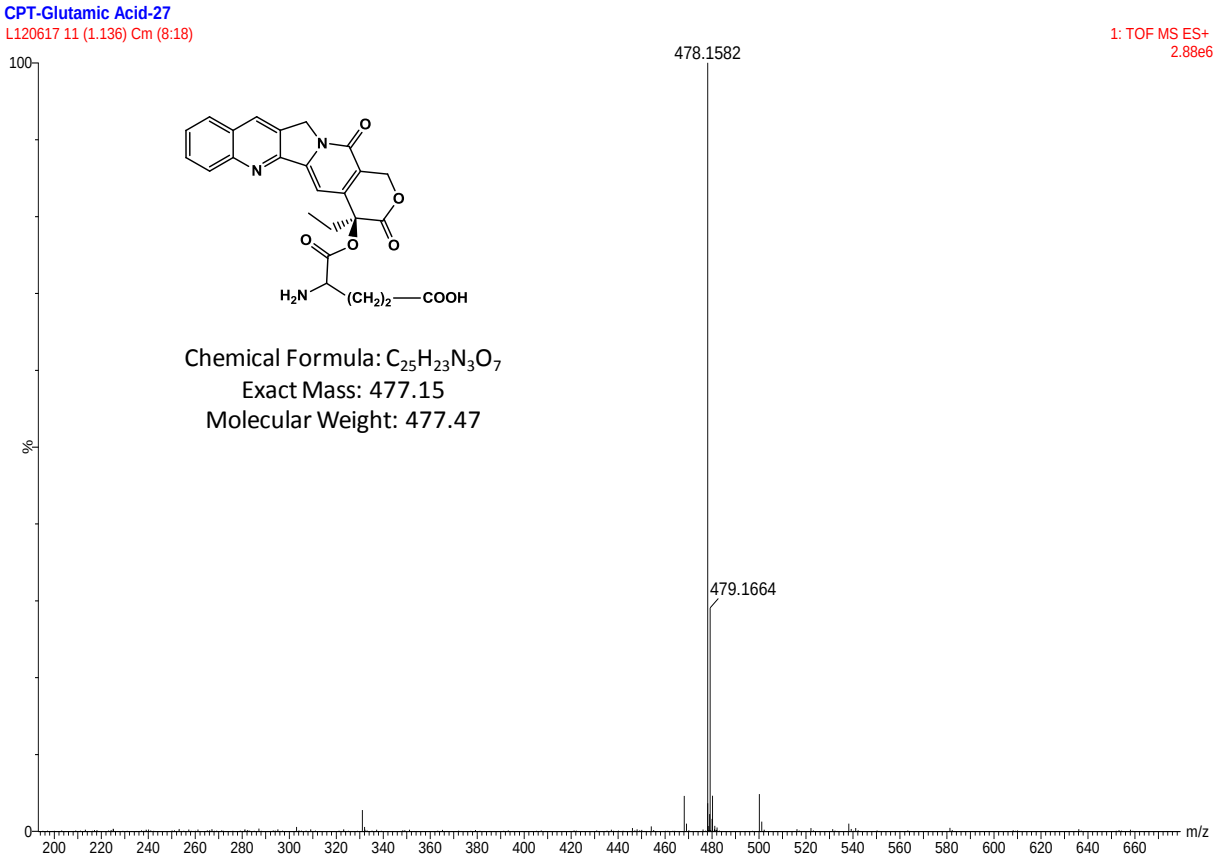

Figure 1. The ESI-MS spectrum of CPT-Glu after purification with MH^{+} of m/z 478.15.

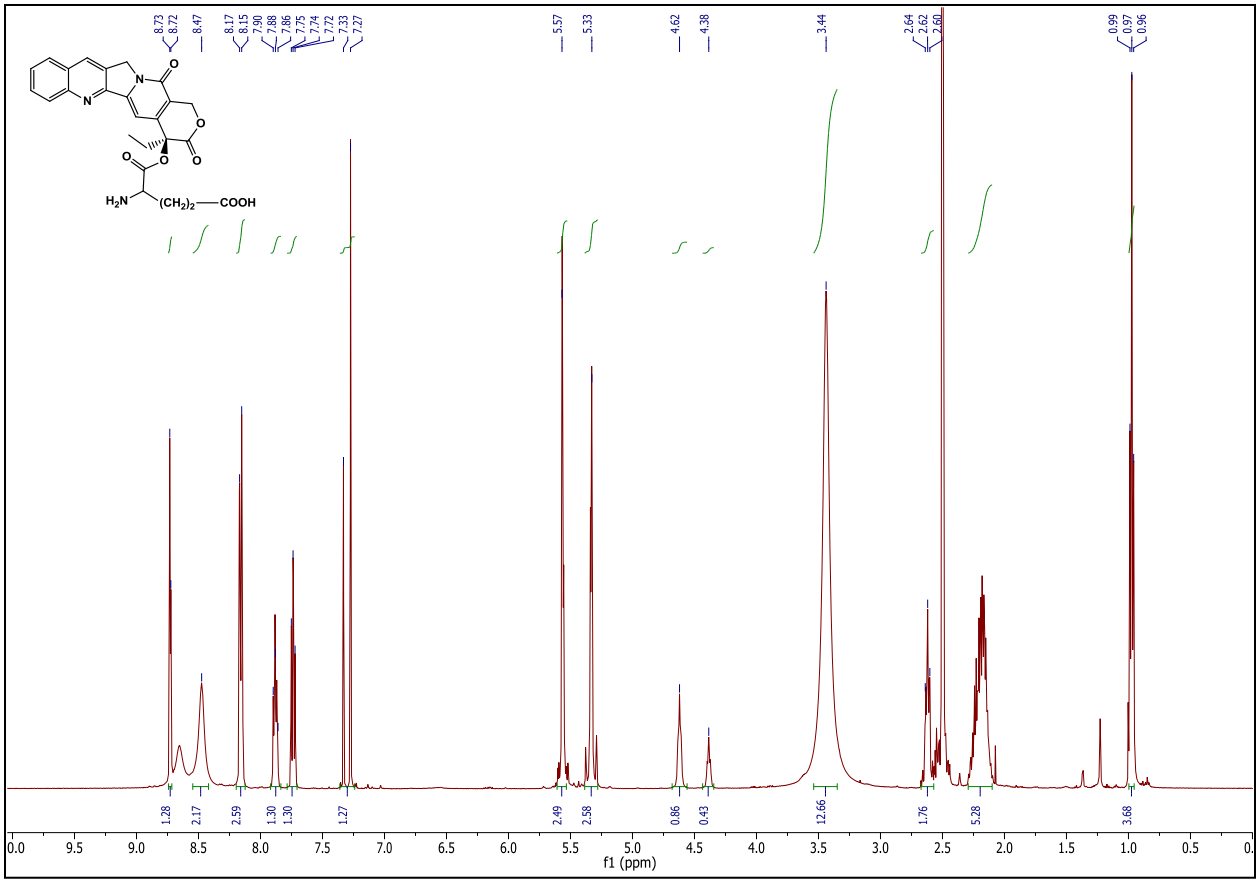

Figure 2. The ^{1}H-NMR spectrum of pure CPT-Glu in DMSO-d6.

3.3. Detection and Analysis of Camptothecin and CPT-Glutamate by LC-MS/MS

Standard solutions of CPT, CPT-Glu, and SN-38 (IS) were first analyzed using MS and MS/MS to obtain their precursor and product ions, respectively, for their use in multiple reaction monitoring (MRM) mode. ESI full scan spectra produced dominant peaks of MH^+ at m/z 349.1 for CPT, m/z 478.1 for CPT-Glu and m/z 393.1 for SN-38. LC-MS/MS collision induced dissociation of each MH^+ ions to produce major fragments at m/z 305.2 for CPT (Figure 3), 331.0 for CPT-Glu (Figure 4) and 349.1 for IS (Figure 5). Product ions from both CPT and SN-38 were derived from the loss of CO_2 (–44 mU) from the lactone ring [29]. The CPT fragment of

CPT-Glu was generated via the loss of L-glutamic amino acid residue (–147 mU) upon ester bond cleavage.

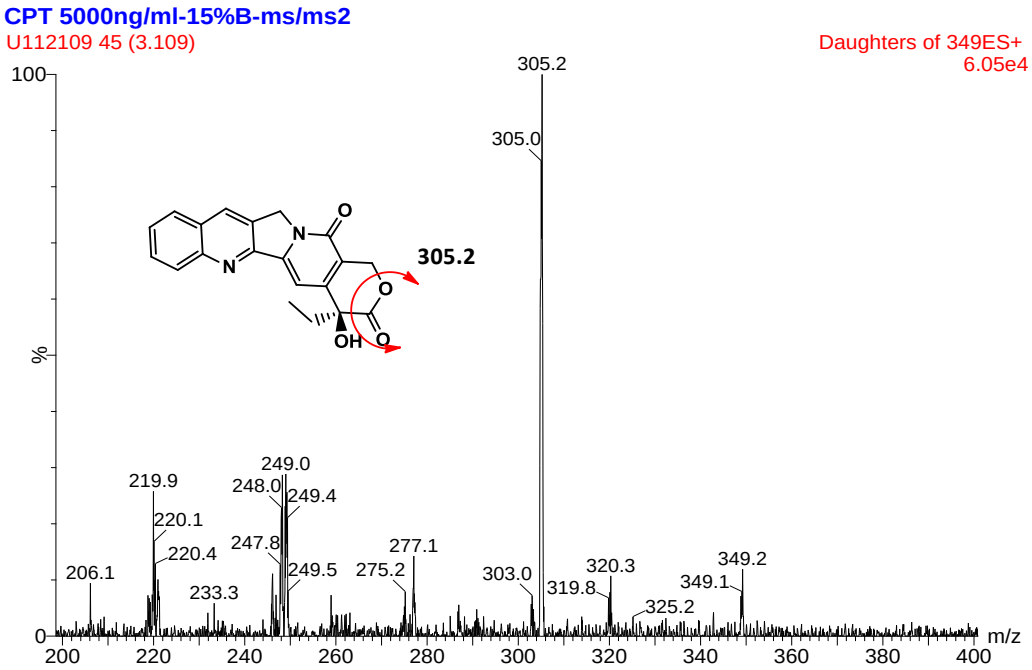

Figure 3. Mass spectrum of daughter ion scan of CPT. The product ion of CPT (m/z 349.1) was subjected to collision induced dissociation to produce daughter ion (dominant peak) at m/z 305.2. These ions will be selected for use in MRM [29].

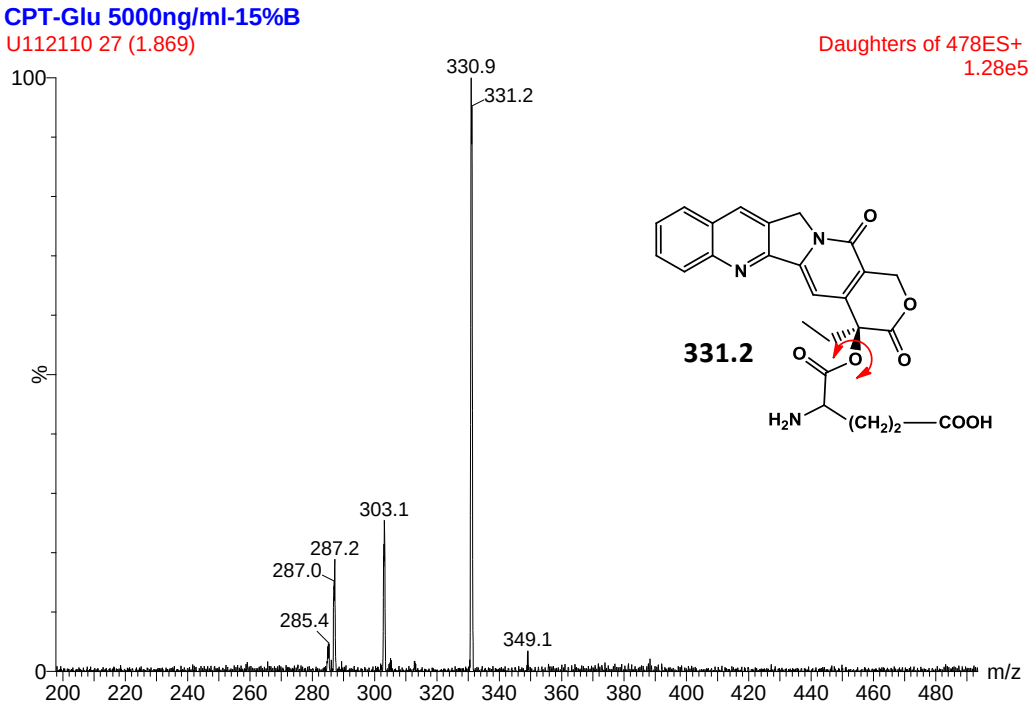

Figure 4. Mass spectra scan for the daughter ion of CPT-Glu. Product ion of CPT-Glu (m/z 478) was subjected to collision induced dissociation to produce dominant peak (daughter ion) at m/z 331.2. Both ions will be selected for use in MRM.

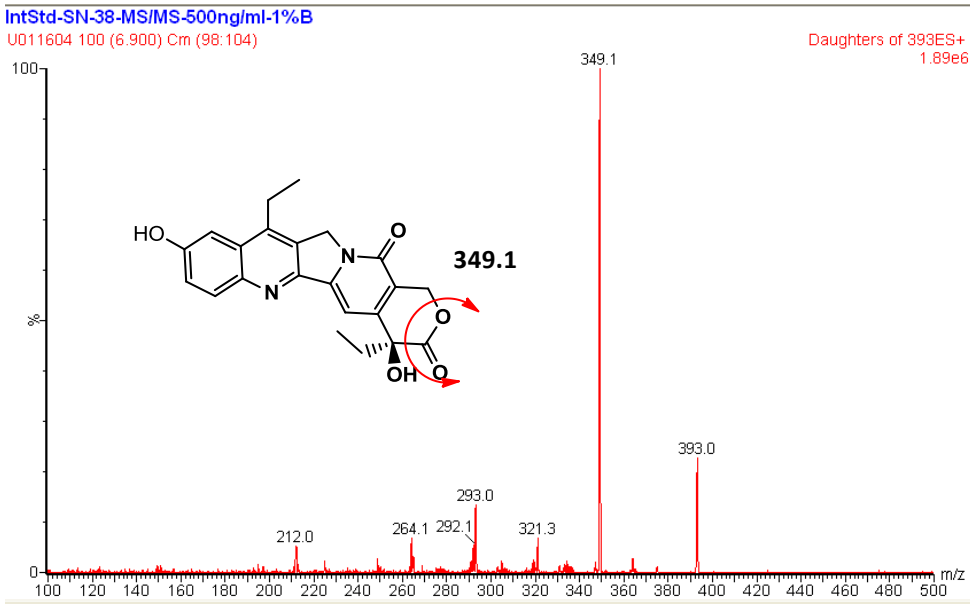

Figure 5. Mass spectra scan for daughter ion of internal standard SN-38 (m/z = 393.0). Collision induced dissociation produced dominant peak at m/z 349.1. The ions will be selected for use in MRM [29].

The precursor and product ions obtained from MS/MS spectra were used to generate transitions for their use in MRM. The transition pairs used in MRM detection for each analyte were *m/z* 349.1 >> 305.2 for CPT, 478.1 >> 331.0 for CPT-Glu and 393.1 >> 349.1 for IS (SN-38). Figure 6 represents MRM chromatograms of rat brain tissue before and after the *in-situ* brain perfusion of CPT-Glu. Analysis of brain tissues of untreated rats showed that there was no endogenous interference at the retention times of CPT, CPT-Glu, and SN-38 (Figure 6a). MRM chromatogram of CPT-Glu resulted in the elution of two peaks at 1.93 and 2.04 min (Figure 6b), which indicated the presence of a diastereomer that was generated during the esterification reaction. Both peaks were summed to represent the total amount of CPT-Glu detected. CPT-Glu was hydrolyzed to produce CPT in the brain by esterases (Figure 6c). The internal standard (IS) spiked into tissue homogenate after extraction (Figure 6d) was successfully separated from other analytes.

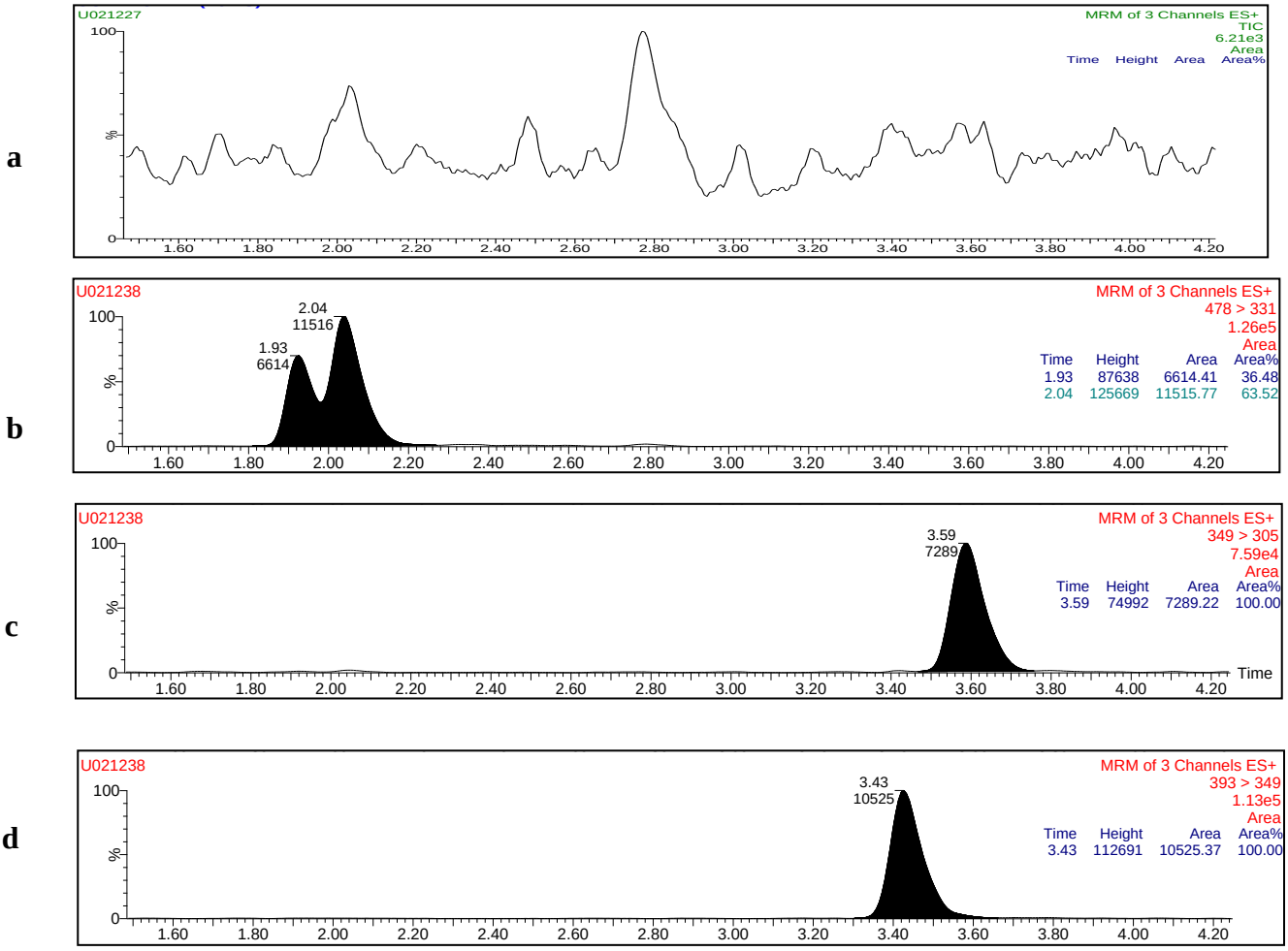

Figure 6. MRM Chromatograms of brain tissue homogenates for CPT, CPT-Glu, and SN-38. (a) brain tissue extract from an untreated rat showing no interfering peaks for CPT, CPT-Glu and SN-38 at their respective retention times (b) brain tissue extract from rats detecting CPT-Glu (1.93 and 2.04 min) after *in-situ* brain perfusion (c) hydrolyzed product CPT (3.59 min) detected in brain homogenate after perfusion studies (d) tissue homogenate spiked with IS, SN-38 (25ng/mL)

3.3.1. Extraction Efficiency of CPT and CPT-Glu

In order to quantitatively determine the amount of drug in the brain, extraction efficiencies were calculated for CPT and CPT-Glu in the brain homogenate using previously published methods with minor modifications [30]. CPT recovery values from brain were found to be around 86% to 92% and CPT-Glu values were around 99–100% (Table 1). These values are ideal for recovery of drugs from tissues where the analysis can be hindered due to high degree of protein-drug binding. The recoveries for CPT and CPT-Glu were determined by the ratio of peak area of the analyte spiked before extraction and known concentration(s) spiked after extraction.

Calibration curves for CPT and CPT-Glu were constructed in biological matrices (brain and plasma) to determine the limit of detection (LOD), limit of quantification (LOQ), linearity and range (Table 2). The standards for CPT and CPT-Glu were ranged around 1–500 ng/mL and 50–500 ng/mL, respectively. The calculated LOD and LOQ for CPT in solvent and biological matrices ranged around 0.25–2.4 ng/mL and 0.78–7.9 ng/mL, respectively. CPT-Glu provided slightly higher values of LOD and LOQ, which were around 17 and 57 ng/mL, respectively. Both analytes provided good linear response with regression values of 0.99.

Table 1. Extraction Recovery of CPT and CPT-Glu from homogenized rat brain

Analyte	Nominal Concentration (ng/mL)	Measured concentration (ng/mL)	Extraction recovery (%)
CPT	5	4.58	92
	50	48.03	96
	250	214.57	86
CPT-GLU	50	49.57	99.1
	100	99.01	99
	250	251.08	100.4

Table 2. Regression Analysis of Calibration Curves, limits of detection (LOD), limits of quantification for CPT and CPT-Glu in solvent, plasma and brain homogenate

Analyte	Matrix	Range (ng/mL)	Correlation coefficient (r^2)	LOD (ng/mL)	LOQ (ng/mL)
CPT	Solvent	1-500	0.9983	2.4	7.9
	Plasma	1-500	0.9984	1.2	3.7
	Brain	5-500	0.9997	0.25	0.78
CPT-GLU	Solvent	50-500	0.9983	13.4	45
	Brain	50-500	0.9996	17	57

3.4. Enhancing Paracellular Transport of Camptothecin-Glutamate in Brain Perfusion Model

The ability of HAV6 peptide to improve the paracellular transport of CPT-Glu across the BBB was evaluated using *in-situ* brain perfusion model (Figure 7). CPT-Glu was delivered to the brain of Sprague Dawley rats at 10 mg/kg for 4 min in the absence (control) and presence of 1.0 mM HAV6 peptide. Although there is some trend showing increased uptake of CPT-Glu in HAV6 treated rats when compared to control, there is no statistical significance between the two groups (p = 0.128). In total, we were able to detect approximately 498 ng/g drug/brain of CPT-lactone in brain, which represents less 0.020% delivered.

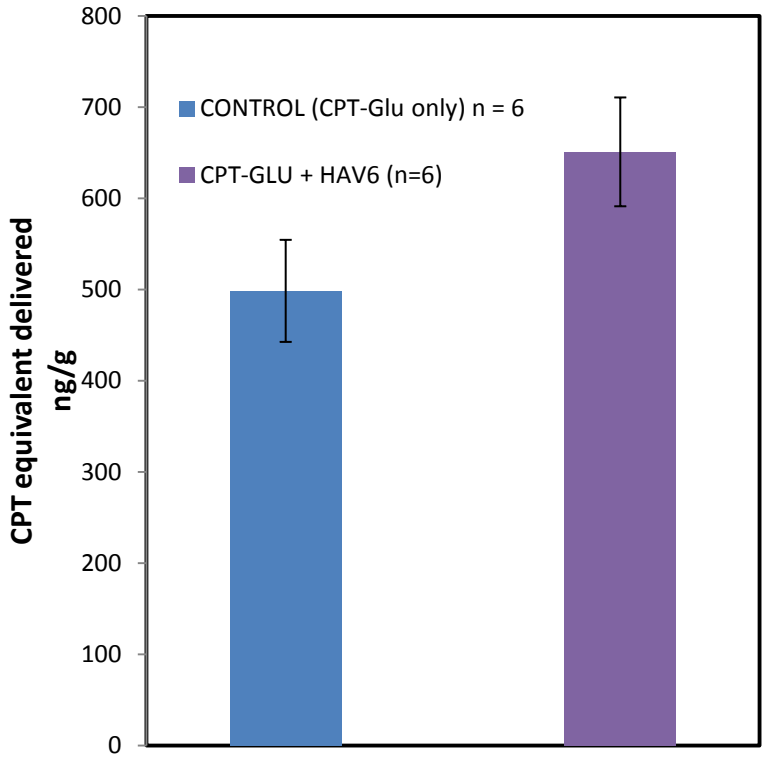

Figure 7. CPT-Glutamate detected in brain after *in-situ* brain perfusion. Rat brains were perfused with 1.0 mM HAV6 peptide at a flow rate of 5 ml/min prior to the delivery of CPT-Glutamate (10 mg/kg rat). Data was represented as mean ± S.E with p = 0.128. Control and CPT-Glu + HAV6 was N = 6.

4. DISCUSSIONS

The treatment of brain tumors by conventional methods such as chemotherapy has become a significant challenge; therefore, there has been a need for other non-invasive drug delivery systems to improve delivery of anticancer drugs to the brain [31]. CPT has been considered a promising drug in treating cancer due to its specificity in targeting DNA-topoisomerase-I, which is upregulated in many cancers. For example, CPT was delivered intraperitoneally at 5 and 10 mg/kg to athymic nude mice bearing human gastric adenocarcinomas (WIL and TOR) for 3 days a week over a 3 week period [32]. The results showed that CPT significantly inhibited the growth of WIL and TOR gastric tumors resulting in the increase in expression of cell cycle inhibitor p21 and the decrease in expression of the apoptosis inhibitor Bcl-2 [32]. Unfortunately, CPT's success as a potential therapeutic drug was limited due to solubility and instability of the lactone ring, which is crucial for biological activity.

CPT has been modified over the years to improve its physical-chemical properties while preserving its antitumor potency. The pentacyclic ring structure in CPT was suggested to be one of the most important structural features of the drug. Typically, modifications made along the A–D rings have been carried our to improve water solubility and provide the necessary framework for DNA interaction [33-35]. It should be noted that the lactone E-ring is essential for interaction with the amino acid residues of topoisomerase-I enzyme and is therefore considered an important element of all CPT derivatives [33, 36-38]. Topotecan (Hycamtin®), an FDA approved CPT analog is currently being used for treating patients with colon, lung, ovarian and brain cancers [39, 40]. The success of topotecan was stemmed from the modification of the benzene ring "A" located in the pentacyclic structure of CPT. However, research has shown that covalent modification of CPT by esterification of the alcohol at the 20-position carbon stabilizes

the lactone ring at physiological pH, preventing the loss of activity associated with lactone ring opening [13, 41].

Our approach to address CPT chemical stability and water solubility problems is by conjugating L-glutamic acid at the 20-position of the lactone ring via an ester bond that will (a) enhance water solubility, (b) stabilize lactone ring during delivery, and (c) efficiently release the unmodified CPT via ester bond hydrolysis by esterases. Liehr *et al*. have investigated stability of CPT and propionate ester derivates in mouse and human plasma [42]. After 4 hours of incubation in phosphate-buffered saline solution containing 4% human plasma, they observed no detectable hydrolysis of the lactone ring in the propionate esters [42]. In contrast, the lactone ring in CPT was rapidly hydrolyzed to the open carboxylate form with a half-life of 11 min when incubated under the same conditions. This result suggests that propionate esters increased the stability of the lactone ring [15, 42-44]. Further investigation revealed that the ester chain in the vicinity of the lactone moiety inhibits albumin binding and makes the conjugate more resistant to hydrolysis [42]. Similarly, we can speculate that our CPT-Glu is more stable than the free CPT. In addition to improved stability, conjugation of L-glutamic acid improved CPT solubility more than 400-fold.

Once the highly soluble CPT-Glu conjugate was synthetized, it was administered with the HAV6 peptide in an *in-situ* brain perfusion model to enhance its brain delivery. Analysis and quantification of CPT-Glu and its metabolites in the brain were done using LC-MS/MS. Here, we have successfully developed and validated a sensitive and selective LC-MS/MS method that could quantify CPT-Glu and CPT in the rat brain tissue. The method development began with the determination of product ions using a full-scan mass spectrometry that detects CPT-Glu and CPT in the brain extracts. Full scan spectra of all analytes were generated using electrospray

ionization (ESI) positive ion mode in a solvent system consisting of 50:50 acetonitrile and water with addition of 0.1% formic acid to provide a higher degree of ionization. The use of electrospray provides high sensitivity with low limits of detection and quantification for analytes. This was found to be an important aspect of analysis of drug molecules in biological matrices. CPT, CPT-Glu, and SN-38 produced protonated molecular ion peaks as theoretically calculated. The SN-38 (IS) was spiked in all matrices prior to introduction to LC-MS/MS as a control for HPLC injection and ionization variability. These values were then selected for the next step in the method development.

MS/MS spectra generated after a full scan spectra were used for structural characterization of all analytes. This is important because it ensures selectivity of our method. Selectivity is the ability of an analytical method to differentiate and quantify an analyte of interest in a complex sample such as biological matrix. MS/MS fragmentations of the molecule not only produce structural detail based on a specific mass loss but provide the ability to distinguish analytes despite having the same molecular weight as endogenous compounds. When CPT, CPT-Glu, and SN-38 were subjected to collision induced dissociation (CID), the applied energy fragmented the lactone ring removing the CO_2 residue from both CPT and SN-38 molecules producing a stable base peak (daughter ion) at m/z 305.2 and 349.1, respectively. CPT-Glu produced a daughter ion of m/z 331.1 when analyzed under the same conditions. This fragment occurred from cleavage of the ester bond at the 20-position of the CPT lactone ring. Comparison of the fragmentation pattern of CPT-Glu (*m/z* 478.1 >> *m/z* 331.1) to that of CPT (*m/z* 349.1 >> *m/z* 305.2) showed that the fragmentation of CPT-Glu did not involve the lactone ring, suggesting that the addition of the L-glutamic acid residue to CPT offers some lactone ring stability.

After method development, the next step was validation. To do this, quality control (QC) samples were used to check for accuracy, precision, sensitivity, linearity of calibration curves, matrix effects, recovery, stability, and reproducibility according to the FDA guidance for bioanalytical method validation over a concentration range of 0–500 ng/mL [45]. CPT and CPT-Glu were quantitatively determined from peak areas calculated after the MRM scanning. CPT was quantified in brain homogenates at concentrations as low as 5 ng/mL with LOD at 0.25 ng/mL. CPT-Glu had slightly higher LOQ and LOD of 57 ng/mL and 17 ng/mL, respectively. It is possible that there was suppression of ionization of CPT-Glu under these LC-MS/MS conditions and could have led to low sensitivity of the CPT-Glu detection. All of our QC samples were highly reproducible with minimal deviation between runs and had coefficient of variations between 0.99% and 14.17 %. This indicates that this method is precise and accurate. We observed good linearity over the studied concentration range with $R^2 = 0.9$ or better.

The extraction recoveries of CPT and CPT-Glu from brain tissue homogenates were excellent with more than 86% efficiency over concentrations ranging from 1–500 ng/mL. The acetonitrile precipitation was used to remove interfering endogenous proteins as well as taking advantage of the high solubility the CPT and CPT-Glu in organic solvent. There are numerous literature reports to indicate that CPT hydrolyses is rapid in blood and tissue samples to produce CPT-carboxylate, which is an inactive form of the drug that binds HSA at high affinity. However, addition of phosphate buffer pH 3.0 (acidic extraction) allows for reversal of lactone hydrolysis. Thus, phosphate buffer pH 3.0 was added into the extraction procedure to ensure determination for total amount of drug delivered in lactone form. All the above taken together indicate that our LC-MS/MS method was robust and could be used for quantification of CPT and CPT-Glu after the *in-situ* brain perfusion.

To improve the delivery of CPT across the BBB, our studies explored synthetic peptides that can modify the BBB pathways to improve CPT-Glu uptake. The *in-situ* brain perfusion technique was used as a model to investigate the efficacy of our HAV6 peptide in modulating the BBB. Extensive research of this peptide in the *in-vitro*, *in-situ*, and *in-vivo* BBB models have shown that this peptide was effective in improving the delivery of small molecules and drugs to the brain [9, 18, 21, 22]. To take this proof-of-concept one step further, we introduced an anticancer drug conjugate in combination with a non-label LC-MS/MS technique that can monitor our conjugate and its metabolites. CPT-Glu was successfully delivered and detected in the brain using the *in-situ* brain perfusion technique. The total drug delivered to the brain was represented by the sum of all conjugate forms and metabolites. Perfusion of the brain with 1.0 mM HAV6 linear peptide prior to delivery of CPT-Glu increased the uptake of the conjugate by approximately 1.30-fold when compared to vehicle control. However, statistical calculations revealed that the comparison of CPT-Glu uptake in the presence and absence of peptide has a *p*-value of 0.128, which is higher than a significant *p*-value of less than 0.05. One of the reasons why we observed no significant increase in CPT-Glu uptake into the brain could be due to the instability of CPT-Glu ester bond during delivery. The perfusion studies were conducted in a buffered saline solution that mimics physiological conditions (pH and salt concentrations) of whole blood and there is a possibility that our conjugate hydrolyzes to CPT thereby decreasing the total CPT-Glu delivered to the brain. Also, the high prevalence of esterases in the BBB could be another contributing factor to the instability of our formulation and therefore the lack of significant enhancement in the delivery of CPT. In the future, studies will be focused on the use of linkers that are more stable than the ester linker used here. The ideal linker should be stable

during formulation and the delivery process but also labile enough to release the active CPT form once in the brain.

5. CONCLUSIONS

Our data demonstrated that we have successfully improved the physical-chemical properties of CPT through conjugation of L-glutamic acid. This modification improved CPT solubility more than 400-fold making our conjugate easier to formulate and deliver. Despite evidence of CPT-Glu diastereomers, both forms were successfully delivered to the brain using *in-situ* rat brain perfusion technique. The acidic extraction method developed was simultaneously able to extract CPT-Glu along with its hydrolyzed product CPT from brain tissue homogenates. This method also provided high extraction recoveries of our drug from the brain (92–100%). The development of a sensitive and selective LC-MS/MS method was successful in identifying and quantifying our CPT-Glu conjugate and it's metabolites in brain tissue producing detection limits as low as 0.25 ng/mL. In the future, a longer duration of peptide incubation and a higher concentration of CPT-Glu will be delivered in the *in-situ* rat brain perfusion model to evaluate the effect of HAV6 peptide in enhancing the brain delivery of CPT.

6. REFERENCES

1. Pardridge, W.M., *Alzheimer's disease drug development and the problem of the blood-brain barrier.* Alzheimers Dement, 2009. **5**(5): p. 427-32.
2. De Bock, M., et al., *Endothelial calcium dynamics, connexin channels and blood-brain barrier function.* Prog Neurobiol, 2013. **108**: p. 1-20.
3. Ballabh, P., A. Braun, and M. Nedergaard, *The blood-brain barrier: an overview: structure, regulation, and clinical implications.* Neurobiol Dis, 2004. **16**(1): p. 1-13.
4. Di, L., H. Rong, and B. Feng, *Demystifying brain penetration in central nervous system drug discovery. Miniperspective.* J Med Chem, 2013. **56**(1): p. 2-12.
5. Abbott, N.J., et al., *Structure and function of the blood-brain barrier.* Neurobiol Dis, 2010. **37**(1): p. 13-25.
6. Bicker, J., et al., *Blood-brain barrier models and their relevance for a successful development of CNS drug delivery systems: a review.* Eur J Pharm Biopharm, 2014. **87**(3): p. 409-32.
7. Scherrmann, J.M., *Drug delivery to brain via the blood-brain barrier.* Vascul Pharmacol, 2002. **38**(6): p. 349-54.
8. Wolburg, H. and A. Lippoldt, *Tight junctions of the blood-brain barrier: development, composition and regulation.* Vascul Pharmacol, 2002. **38**(6): p. 323-37.
9. Sinaga, E., et al., *Increasing paracellular porosity by E-cadherin peptides: discovery of bulge and groove regions in the EC1-domain of E-cadherin.* Pharm Res, 2002. **19**(8): p. 1170-9.
10. Tomicic, M.T. and B. Kaina, *Topoisomerase degradation, DSB repair, p53 and IAPs in cancer cell resistance to camptothecin-like topoisomerase I inhibitors.* Biochim Biophys Acta, 2013. **1835**(1): p. 11-27.
11. Tsai, T.H., et al., *Measurement and pharmacokinetics of unbound 20(S)-camptothecin in rat blood and brain by microdialysis coupled to microbore liquid chromatography with fluorescence detection.* J Chromatogr A, 2000. **870**(1-2): p. 221-6.
12. Saetern, A.M., et al., *Effect of hydroxypropyl-beta-cyclodextrin-complexation and pH on solubility of camptothecin.* Int J Pharm, 2004. **284**(1-2): p. 61-8.
13. Fox, M.E., et al., *Synthesis and in vivo antitumor efficacy of PEGylated poly(l-lysine) dendrimer-camptothecin conjugates.* Mol Pharm, 2009. **6**(5): p. 1562-72.
14. Deshmukh, M., et al., *A series of alpha-amino acid ester prodrugs of camptothecin: in vitro hydrolysis and A549 human lung carcinoma cell cytotoxicity.* J Med Chem, 2010. **53**(3): p. 1038-47.
15. Mi, Z. and T.G. Burke, *Differential interactions of camptothecin lactone and carboxylate forms with human blood components.* Biochemistry, 1994. **33**(34): p. 10325-36.
16. Scott, D.O., D.S. Bindra, and V.J. Stella, *Plasma pharmacokinetics of lactone and carboxylate forms of 20(S)-camptothecin in anesthetized rats.* Pharm Res, 1993. **10**(10): p. 1451-7.
17. Ziomkowska, B., et al., *Deactivation rate of camptothecin determined by factor analysis of steady-state fluorescence and absorption spectra.* Optica Applicata, 2006. **36**(1): p. 137-146.
18. Makagiansar, I.T., et al., *Improving the selectivity of HAV-peptides in modulating E-cadherin-E-cadherin interactions in the intercellular junction of MDCK cell monolayers.* Pharm Res, 2001. **18**(4): p. 446-53.

19. Lutz, K.L. and T.J. Siahaan, *Modulation of the cellular junction protein E-cadherin in bovine brain microvessel endothelial cells by cadherin peptides.* Drug Delivery, 1997. **4**(3): p. 187-193.
20. Pal, D., K.L. Audus, and T.J. Siahaan, *Modulation of cellular adhesion in bovine brain microvessel endothelial cells by a decapeptide.* Brain Res, 1997. **747**(1): p. 103-13.
21. Kiptoo, P., et al., *Enhancement of drug absorption through the blood-brain barrier and inhibition of intercellular tight junction resealing by E-cadherin peptides.* Mol Pharm, 2011. **8**(1): p. 239-49.
22. On, N.H., et al., *Modulation of Blood-Brain Barrier Permeability in Mice Using Synthetic E-Cadherin Peptide.* Mol Pharm, 2014. **11**(3): p. 974-981.
23. Norbedo, S., et al., *Synthesis of 6-amino-6-deoxyhyaluronan as an intermediate for conjugation with carboxylate-containing compounds: application to hyaluronan-camptothecin conjugates.* Carbohydrate Research, 2009. **344**(1): p. 98-104.
24. Henne, W.A., et al., *Synthesis and activity of a folate peptide camptothecin prodrug.* Bioorganic & Medicinal Chemistry Letters, 2006. **16**(20): p. 5350-5355.
25. Ketola, R.A. and T. Mauriala, *Mass spectrometric tools for cell and tissue studies.* European Journal of Pharmaceutical Sciences, 2012. **46**(5): p. 293-314.
26. Bhatt, R.V., Peter De; Klein, Peter J.; Tulinsky, John; Lewis, Robert A.; Singer, Jack W., *Polyglutamic acid-camptothecin conjugates and methods of preparation*, 2006, Cell Therapeutics Inc: USA. p. 1-26.
27. Greenwald, R.B., A. Pendri, and H. Zhao, *Stereoselective acylation of 20-(S)-camptothecin with amino acid derivatives using scandium triflate/DMAP.* Tetrahedron-Asymmetry, 1998. **9**(6): p. 915-918.
28. Takasato, Y., S.I. Rapoport, and Q.R. Smith, *An in situ brain perfusion technique to study cerebrovascular transport in the rat.* Am J Physiol, 1984. **247**(3 Pt 2): p. H484-93.
29. Khan, S., et al., *A simple and sensitive LC/MS/MS assay for 7-ethyl-10-hydroxycamptothecin (SN-38) in mouse plasma and tissues: application to pharmacokinetic study of liposome entrapped SN-38 (LE-SN38).* J Pharm Biomed Anal, 2005. **37**(1): p. 135-42.
30. Martins, S.M., et al., *Development and validation of a simple reversed-phase HPLC method for the determination of camptothecin in animal organs following administration in solid lipid nanoparticles.* J Chromatogr B Analyt Technol Biomed Life Sci, 2012. **880**(1): p. 100-7.
31. Martins, S., et al., *Brain delivery of camptothecin by means of solid lipid nanoparticles: formulation design, in vitro and in vivo studies.* Int J Pharm, 2012. **439**(1-2): p. 49-62.
32. Litvak, D.A., et al., *Targeting molecular pathways with camptothecin as novel therapy for gastric cancer.* Journal of Gastrointestinal Surgery, 1999. **3**(6): p. 618-624.
33. Huang, Q., L. Wang, and W. Lu, *Evolution in medicinal chemistry of E-ring-modified Camptothecin analogs as anticancer agents.* Eur J Med Chem, 2013. **63**: p. 746-57.
34. Wani, M.C., et al., *Plant antitumor agents. 18. Synthesis and biological activity of camptothecin analogues.* J Med Chem, 1980. **23**(5): p. 554-60.
35. Fattorusso, E.T.-S., O, *Modern Alkaloids: Structure, Isolation, Synthesis and Biology*. 2007: Wiley-VCH.
36. Redinbo, M.R., et al., *Crystal structures of human topoisomerase I in covalent and noncovalent complexes with DNA.* Science, 1998. **279**(5356): p. 1504-13.

37. Fan, Y., et al., *Molecular modeling studies of the DNA-topoisomerase I ternary cleavable complex with camptothecin.* J Med Chem, 1998. **41**(13): p. 2216-26.
38. Kerrigan, J.E. and D.S. Pilch, *A structural model for the ternary cleavable complex formed between human topoisomerase I, DNA, and camptothecin.* Biochemistry, 2001. **40**(33): p. 9792-8.
39. Baczek, T., et al., *Topotecan exposure estimation in pediatric acute myeloid leukemia supported by LC-MS-based drug monitoring and pharmacokinetic analysis.* Journal of Pharmaceutical and Biomedical Analysis, 2012. **70**: p. 330-336.
40. Li, N., et al., *Absolute bioavailability studies of a new oral topotecan formulation in Chinese patients using UHPLC-MS/MS.* Journal of Pharmaceutical and Biomedical Analysis, 2013. **76**: p. 252-256.
41. Zhao, H., et al., *20-O-acylcamptothecin derivatives: Evidence for lactone stabilization.* Journal of Organic Chemistry, 2000. **65**(15): p. 4601-4606.
42. Liehr, J.G., et al., *Pharmacology of camptothecin esters.* Ann N Y Acad Sci, 2000. **922**: p. 216-23.
43. Burke, T.G. and Z.H. Mi, *The Structural Basis of Camptothecin Interactions with Human Serum-Albumin - Impact on Drug Stability.* Journal of Medicinal Chemistry, 1994. **37**(1): p. 40-46.
44. Burke, T.G. and Z.H. Mi, *Preferential Binding of the Carboxylate Form of Camptothecin by Human Serum-Albumin.* Analytical Biochemistry, 1993. **212**(1): p. 285-287.
45. *Guidance for Industry - Bioanalytical Method Validation*, May 2001, U.S. Department of Health and Human Services; Food and Drug Administration; Center for Drug Evaluation and Research (CDER); Center for Veterinary Medicine (CVM). p. 1-25.